# Chromatographic Resolution of a Diastereomeric Mixture of Tris(*trans*-1,2-diaminocyclohexane)cobalt(III) by Bis(μ-tartrato)diantimonate(III) Anion and Association Modes Found in Their Diastereomeric Salts

**Tsutomu Mizuta, Ken-ichi Sasaki, Hiromi Yamane, Katsuhiko Miyoshi,* and Hayami Yoneda†**

Department of Chemistry, Faculty of Science, Hiroshima University, Kagamiyama, Higashi-Hiroshima 739-8526

†Department of Fundamental Science, Okayama University of Science, 1-1 Ridaicho, Okayama 700-0005

(Received December 12, 1997)

The chromatographic resolution of a diastereomeric mixture of $\Lambda$-*ob*$_3$-, $\Delta$-*ob*$_3$-, $\Lambda$-*lel*$_3$-, and $\Delta$-*lel*$_3$-$[Co(chxn)_3]^{3+}$ (chxn = *trans*-1,2-diaminocyclohexane) was carried out on an ion-exchange column using bis(μ-tartrato)diantimonate(III), $[Sb_2(d\text{-tart})_2]^{2-}$ as a resolving reagent. The resulting elution order of $\Lambda$-*ob*$_3$ > $\Lambda$-*lel*$_3$ > $\Delta$-*lel*$_3$ > $\Delta$-*ob*$_3$ was interpreted on the basis of an association model in which lone-pairs on three oxygen atoms of $[Sb_2(d\text{-tart})_2]^{2-}$ form triple hydrogen bonds with three N–H groups directed along the $C_3$-axis of $[Co(chxn)_3]^{3+}$. Since the three N–H groups of the $\Lambda$-*ob*$_3$ isomer have a right-handed helicity, they form the strongest linear hydrogen bonds with the three lone-pairs of $[Sb_2(d\text{-tart})_2]^{2-}$, which are also spirally oriented in the same sense, whereas those of the two *lel*$_3$ isomers having practically no such helicity form weaker hydrogen bonds, and those of the $\Delta$-*ob*$_3$ isomer having the opposite helicity have the hydrogen bonds much damaged. To obtain structural evidence for the above association model, crystal structures of diastereomeric salts, $\Lambda$-*ob*$_3$-$[Co(chxn)_3]X[Sb_2(d\text{-tart})_2]\cdot nH_2O$, $X^- = Cl^-$ (**1**) and $ClO_4^-$ (**2**) have been determined by single-crystal analyses. The crystal data are as follows: **1** is orthorhombic, with a space group $P2_12_12_1$, $Z=4$, $a=10.823(2)$, $b=17.901(7)$, $c=21.477(6)$ Å, $V=4161(2)$ Å$^3$, and $R=0.057$; **2** is monoclinic with a space group $P2_1$, $Z=4$, $a=13.338(2)$, $b=17.119(3)$, $c=18.060(3)$ Å, $\beta=98.31(1)°$, $V=4080(1)$ Å$^3$, and $R=0.049$. In both crystals, $[Sb_2(d\text{-tart})_2]^{2-}$ approaches $\Lambda$-*ob*$_3$-$[Co(chxn)_3]^{3+}$ along the $C_3$-axis of the complex to form multiple hydrogen bonds, as expected, and one of the contact modes found in **2** is close to our proposed association model.

Intermolecular chiral recognition and discrimination phenomena are of widespread interest and profound importance in chemistry and biology. Chiral metal complexes have been utilized to probe such intermolecular interactions, since they have a number of potential advantages in designing steric/electrostatic "lock and key" models.[1] Hydrogen bonding in such models is one of the forces which play a major role in the interaction with the chiral metal complexes. Although a number of models in which a chiral molecule interacts with the complex through the intermolecular hydrogen bonds have been proposed to rationalize chiral-recognition phenomena,[2—4] there are few models which incorporate the directionality of the lone-pair electrons on hydrogen-acceptor atoms.[2g,5] The significance of the directionality in the hydrogen bond has been recognized in view of theoretical calculations,[6] microwave studies on gas-phase dimers,[7] and statistical analyses of hydrogen-bond geometries found in organic crystals.[8] Thus, if the directionality of the lone-pairs is incorporated into the association model, a more specific discrimination will be attained without any recourse to the stereoselective repulsion often invoked.

It is well known that bis(μ-tartrato)diantimonate(III), abbreviated as $[Sb_2(d\text{-tart})_2]^{2-}$, is a versatile resolving reagent for many cationic metal complexes with widely different structures and properties.[9] Especially, it serves as an effective eluent in the chromatographic resolution of octahedral complex cations having amino groups as ligands.[2a,2i,2j,10,11] Since the $[Sb_2(d\text{-tart})_2]^{2-}$ shown in Scheme 1 has many lone-pairs on its $sp^2$- and $sp^3$-hybridized oxygen atoms, it is natural to expect their participation in hydrogen bonds with the N–H groups of the $[Co(N)_6]^{3+}$ complexes. On the basis of such an expectation, we have already proposed an association model in which $[Sb_2(d\text{-tart})_2]^{2-}$ interacts with $[Co(N)_6]^{3+}$-type complexes through its lone-pairs.[2g] However, though many examples of chiral recognition by $[Sb_2(d\text{-tart})_2]^{2-}$ have been successfully interpreted using our model, none of them was designed so that the lone-pair electrons of $[Sb_2(d\text{-tart})_2]^{2-}$ may exhibit the potential ability to recognize the chirality of these complexes.

When the molecular structure of the $[Sb_2(d\text{-tart})_2]^{2-}$ (shown in Scheme 1) is examined in detail, several combinations of the oxygen atoms are seen to be available for the multiple hydrogen bonds. Among them, the three shaded oxygen atoms in Scheme 1 are disposed nicely to a triangular face of $[Co(N)_6]^{3+}$ to form triple hydrogen bonds with the three N–H groups, and $[Sb_2(d\text{-tart})_2]^{2-}$ has four sets of such three oxygen atoms, which are favorably utilized from a statistical point of view. In addition, if the lone-pairs are assumed on these oxygen atoms, the three lone-pairs shown in Scheme 1 are disposed spirally so as to define a right-handed

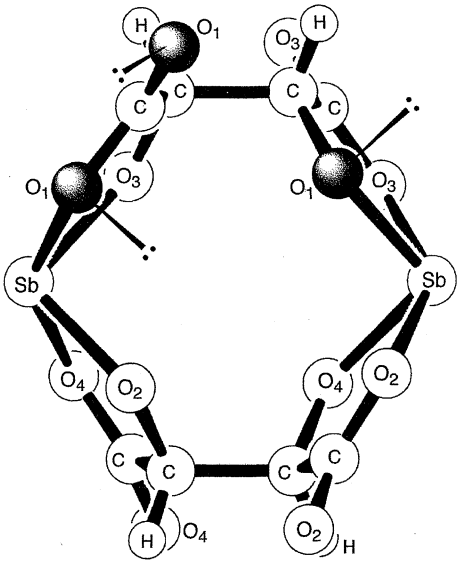


Scheme 1. Molecular structure of $[Sb_2(d\text{-tart})_2]^{2-}$ ion. Three shaded oxygen atoms are used for triple hydrogen bonds. The wedges indicate the directions of lone-pairs on each oxygen atom. Other sets of oxygen atoms are labeled as $O_2$, $O_3$, and $O_4$.

helicity. If these spirally oriented lone-pairs are used, $[Sb_2(d\text{-tart})_2]^{2-}$ forms linear, and thus strong, hydrogen bonds with a complex having the three N–H groups spirally oriented in the same sense. When $\Lambda$-$[Co(en)_3]^{3+}$ assumes an $ob_3$ conformation, as shown in Scheme 2-a, it meets such requirements, (where the *ob* denotes that a C–C bond of a five membered ring lies oblique to the $C_3$-axis of the complex, while the *lel* denotes that it lies parallel to that axis, and the number of the subscript refers to the number of *ob* and *lel* conformers in the complex). However, since the conformation of the en chelate ring is labile, $[Co(en)_3]^{3+}$ is not appropriate to verify our proposal. Thus, a chxn ligand (chxn = *trans*-1,2-diaminocyclohexane) having two chiral centers and a rigid conformation is used as an alternative.

In this study, we employed two pairs of enantiomers of $lel_3$- and $ob_3$-$[Co(chxn)_3]^{3+}$ and their derivatives as target complexes, and investigated the influence of the directionality of the N–H groups on chiral discrimination attained with the helical lone-pairs of $[Sb_2(d\text{-tart})_2]^{2-}$.

## Results and Discussion

**Chromatography of the Diastereomeric Mixture.** Figure 1-a shows a separation profile of the isomers of $[Co(chxn)_3]^{3+}$ on an SP-Sephadex column with aqueous $K_2[Sb_2(d\text{-tart})_2]$ as an eluent. When a mixture of $\Lambda$-$ob_3$-, $\Delta$-$ob_3$-, $\Lambda$-$lel_3$-, and $\Delta$-$lel_3$-$[Co(chxn)_3]^{3+}$ loaded on the top of the column is eluted, all of the isomers are completely separated. The fastest eluted isomer in Fig. 1-a is $\Lambda$-$ob_3$-$[Co(chxn)_3]^{3+}$, followed by $\Lambda$-$lel_3$, $\Delta$-$lel_3$, and $\Delta$-$ob_3$ in this order. Under the present chromatographic conditions, the elution largely depends on the degree of association of the eluent with the complex ions.[2a,12] Therefore, the result shown in Fig. 1-a indicates that the order of the affinity of $[Sb_2(d\text{-tart})_2]^{2-}$ toward the four isomers of $[Co(chxn)_3]^{3+}$ is $\Lambda$-$ob_3$ > $\Lambda$-$lel_3$ > $\Delta$-$lel_3$ > $\Delta$-$ob_3$.

The following assumption concerning an association site of $[Co(chxn)_3]^{3+}$ makes the interpretation of the above elution order possible. Since the $[Co(chxn)_3]^{3+}$ in Chart 1 has three bulky cyclohexane rings disposed in a direction perpendicular to the $C_3$-axis of the complex, large $[Sb_2(d\text{-tart})_2]^{2-}$ inevitably approaches the complex along the $C_3$-axis in order to avoid a steric hindrance from the bulky cyclohexane rings. In addition, since the three N–H groups on the triangular face are available for multiple hydrogen bonds along the $C_3$-axis, this face is considered to be the most probable association site ($C_3$ site) to which the three oxygen atoms of $[Sb_2(d\text{-tart})_2]^{2-}$ form triple hydrogen bonds. Several experimental results are in favor of this interaction mode. For example, Sakaguchi et al. examined a CD-spectral change of the $[Co(N)_6]^{3+}$ complexes upon association with $[Sb_2(d\text{-tart})_2]^{2-}$.[13] They concluded that $[Sb_2(d\text{-tart})_2]^{2-}$ exclusively exerts a $C_3$-axial perturbation on $[Co(chxn)_3]^{3+}$ based on the observed increment in an $A_2$ component of the CD spectrum.

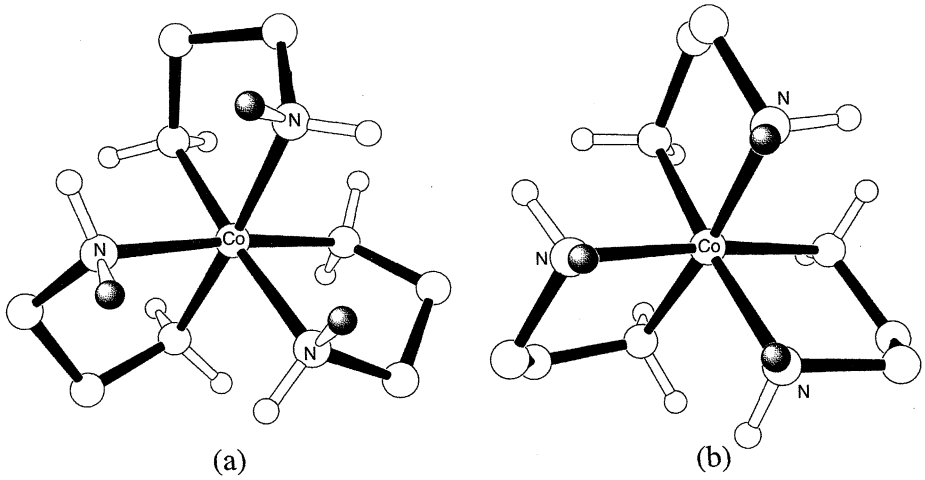


Scheme 2. Molecular structures of $\Lambda$-$ob_3$-$[Co(en)_3]^{3+}$ (a) and $\Lambda$-$lel_3$-$[Co(en)_3]^{3+}$ (b). Three hydrogen atoms on the triangular face are indicated as shaded circles. Hydrogen atoms on carbon atoms are eliminated for clarity.

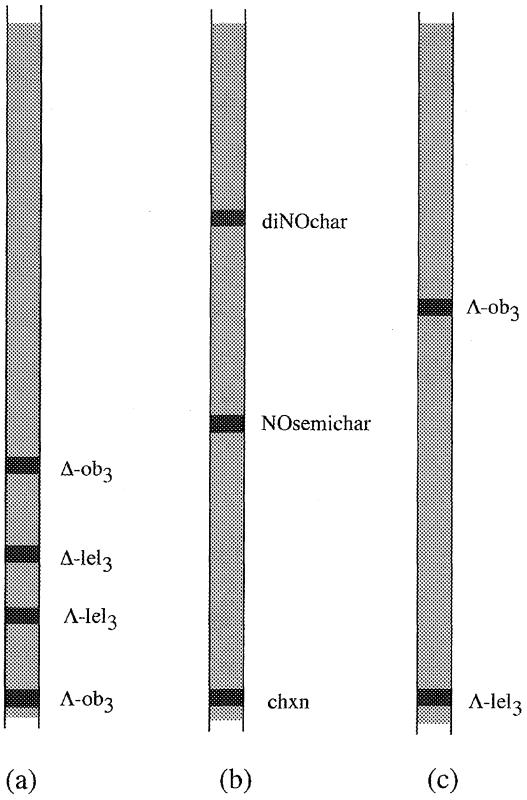


Fig. 1. Chromatographic separation on SP-Sephadex column with eluents $K_2[Sb_2(d\text{-tart})_2]$ aq (a) and (b), and with 0.2 M $Na_2SO_4$ aq (c). Samples: column (a), $\Lambda$-*ob*$_3$-, $\Delta$-*ob*$_3$-, $\Lambda$-*lel*$_3$-, and $\Delta$-*lel*$_3$-$[Co(chxn)_3]Cl_3$; (b), $\Lambda$-*lel*$_3$-$[Co(chxn)_3]Cl_3$; $\Lambda$-$[Co(NOsemichar)]Cl_3$, and $\Lambda$-$[Co(diNOchar)]Cl_3$; (c), $\Lambda$-*ob*$_3$- and $\Lambda$-*lel*$_3$-$[Co(chxn)_3]Cl_3$.

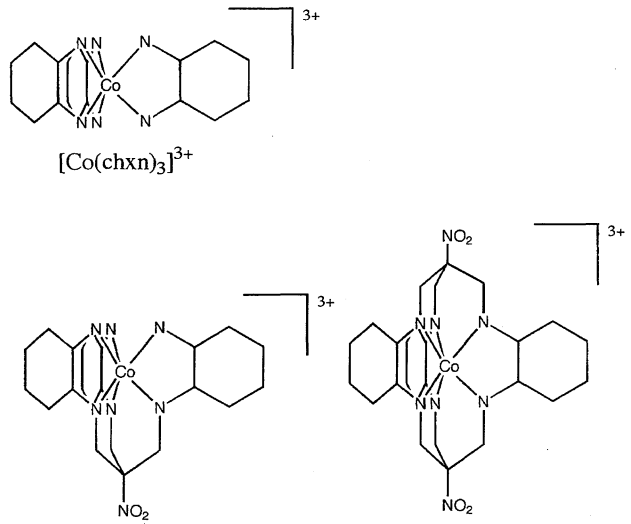


Chart 1.

To confirm the association site further, chromatography was performed using a mixture of $\Lambda$-*lel*$_3$-$[Co(chxn)_3]^{3+}$ and its derivatives, $\Lambda$-$[Co(NOsemichar)]^{3+}$ in which one of the two $C_3$ sites of the parent $[Co(chxn)_3]^{3+}$ was masked by a bulky alkyl cap, and $\Lambda$-$[Co(diNOchar)]^{3+}$ which has the two $C_3$ sites, both being masked (Chart 1).[14] The result of the chromatography is shown in Fig. 1-b, where a mixture of the three complexes were eluted with aqueous $K_2[Sb_2(d\text{-tart})_2]$. $\Lambda$-$[Co(NOsemichar)]^{3+}$ was eluted considerably late after $\Lambda$-*lel*$_3$-$[Co(chxn)_3]^{3+}$, as expected, and $\Lambda$-$[Co(diNOchar)_3]^{3+}$ was much harder to elute. This result strongly supports our association model. In other words, the approach of $[Sb_2(d\text{-tart})_2]^{2-}$ from a direction other than an axial direction suffers a considerable disadvantage in association.

The discussion is now focused on the structural difference in the $C_3$ association sites among the isomers. First of all, it is worth noting that the affinity order of $[Sb_2(d\text{-tart})_2]^{2-}$ toward the $\Lambda$-*ob*$_3$ and $\Lambda$-*lel*$_3$ isomers is opposite to that of common oxo anions;[4e,15] for example, $SO_4^{2-}$ has a greater affinity for the $\Lambda$-*lel*$_3$ isomer, as shown in Fig. 1-c. This is because the N–H groups of the *lel*$_3$ isomer are disposed parallel to the $C_3$-axis (as shown in Scheme 2-b) to form three linear N–H···O hydrogen bonds with the three oxygen atoms of $SO_4^{2-}$, while those of the *ob*$_3$ isomer are inclined relative to the $C_3$-axis, resulting in bent, and therefore weaker, hydrogen bonds.[16] The contrasting result attained with $[Sb_2(d\text{-tart})_2]^{2-}$ suggests that the strength of the hydrogen bond with the $C_3$ site is governed not only by the simple electrostatic interaction, but also by some additional effect; that is, the fitness of the helicity between the three lone-pairs of $[Sb_2(d\text{-tart})_2]^{2-}$ and the three N–H groups. The three N–H groups of the $\Lambda$-*ob*$_3$ isomer are oreinted spirally to form a right-handed helicity, which is the same as that defined by the three lone-pairs of $[Sb_2(d\text{-tart})_2]^{2-}$ (Scheme 1), and thus, these N–H groups form linear and strong hydrogen bonds with $[Sb_2(d\text{-tart})_2]^{2-}$. In contrast, the $\Delta$-*ob*$_3$ isomer forms the weakest hydrogen bonds with $[Sb_2(d\text{-tart})_2]^{2-}$, because it has three N–H groups oriented spirally in the opposite sense; thus it is the least eluted. On the other hand, the N–H groups of the *lel*$_3$ isomer, which are not inclined, thus fit the helical lone-pairs worse than those of the $\Lambda$-*ob*$_3$ isomer. In this way, the elution order shown in Fig. 1-a is reasonably interpreted within the framework of our association model.

Here, the elution order of the two *lel*$_3$ isomers in Fig. 1-a are examined. With regard to the three N–H groups of the $C_3$ site, both of the *lel*$_3$ isomers are similar in structure, and thus form hydrogen bonds that are similar in strength. We have previously discussed that the chiral discrimination of such an enantiomeric pair, $\Lambda$ and $\Delta$, is attained through a stereoselective repulsion.[2g] That is, when $[Sb_2(d\text{-tart})_2]^{2-}$ forms the three hydrogen bonds with the $C_3$ site, its distal carboxylate group is situated between the two chelate rings in association with the $\Lambda$ complex, whereas it experiences a steric hindrance from the one chelate ring in association with the $\Delta$ complex, leading to a faster elution of the $\Lambda$-*lel*$_3$ isomer. There is no doubt that a similar steric repulsion also plays an additional role in the chiral discrimination between the $\Lambda$-*ob*$_3$ and $\Delta$-*ob*$_3$ isomers, thus further improving the efficiency in their chromatographic separation.

**Crystal Structures of Diastereomeric Salts.** To obtain structural support for our association model, crystal-structure

analyses were carried out for diastereomeric salts comprising $\Lambda$-$ob_3$-$[Co(chxn)_3]^{3+}$ and $[Sb_2(d\text{-tart})_2]^{2-}$. Although the preparation of other diastereomeric salts was also tried, the obtained crystals did not have sufficient sizes and qualities for the crystal analysis. We succeeded in structural analyses of the following two diastereomeric salts: $\Lambda$-$ob_3$-$[Co(chxn)_3]$-$Cl[Sb_2(d\text{-tart})_2]\cdot 4.5H_2O$ (**1**) and $\Lambda$-$ob_3$-$[Co(chxn)_3](ClO_4)$-$[Sb_2(d\text{-tart})_2]\cdot 4H_2O$ (**2**). The crystallographic data and the refinement conditions for **1** and **2** are summarized in Table 1, and the atomic coordinates are listed in Tables 2 and 3, respectively.

Figure 2 gives the packing mode of the complex cation and $[Sb_2(d\text{-tart})_2]^{2-}$ in **1** along with the numbering scheme for the respective atoms; the $\Lambda$-$ob_3$-$[Co(chxn)_3]^{3+}$ and the $[Sb_2(d\text{-tart})_2]^{2-}$ alternately pile up along an *a*-axis of a crystal cell to form a column structure, and water molecules and chloride anions are located between the columns to connect them. The structure displayed in Fig. 2 indicates that the two $[Sb_2(d\text{-tart})_2]^{2-}$ ions make a similar contact with the complex along its $C_3$-axis (a vertical direction in the figure) at the upper and lower sides of the complex. The two similar contact modes are named here as *type-I*, and only one of them is drawn as a stereoview in Fig. 3, where the lone-pairs labeled as LA or LB are attached to the $sp^3$- or $sp^2$-hybridized oxy-

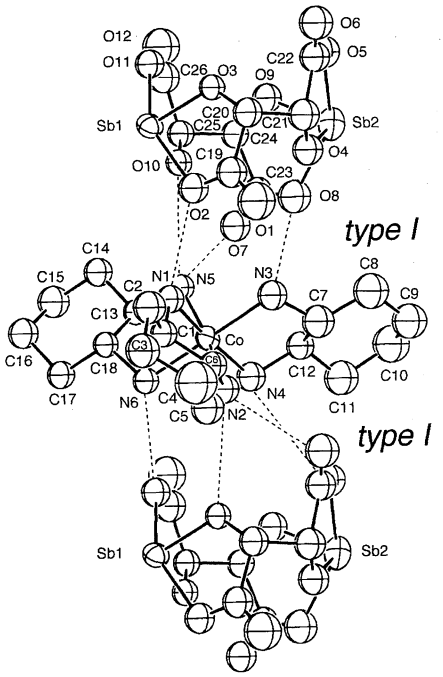


Fig. 2. Drawing of packing mode of $\Lambda$-$ob_3$-$[Co(chxn)_3]^{3+}$ and $[Sb_2(d\text{-tart})_2]^{2-}$ in **1**. The $[Sb_2(d\text{-tart})_2]^{2-}$ at the bottom is of a neighboring asymmetric unit.

Table 1. Crystal Data, Experimental Conditions, and Refinement Details

| Compound | **1** | **2** |
|---|---|---|
| Chemical formula | $C_{26}H_{55}ClCoN_6O_{16.5}Sb_2$ | $C_{26}H_{54}ClCoN_6O_{20}Sb_2$ |
| Formula weight | 1053.64 | 1108.63 |
| Crystal size/mm$^3$ | $0.1\times0.2\times0.4$ | $0.6\times0.5\times0.5$ |
| Unit-cell dimensions: | | |
| *a*/Å | 10.823 (2) | 13.338 (2) |
| *b*/Å | 17.901 (7) | 17.119 (3) |
| *c*/Å | 21.477 (6) | 18.060 (3) |
| $\beta$/° | | 98.31 (1) |
| Volume of unit cell/Å$^3$ | 4161 (2) | 4080 (1) |
| Crystal system | Orthorhombic | Monoclinic |
| Space group | $P2_12_12_1$ (# 19) | $P2_1$ (# 4) |
| *Z* value | 4 | 4 |
| Density:$D_{calc}$/g cm$^{-3}$ | 1.68 | 1.80 |
| Linear absorption coefficient/cm$^{-1}$ | 18.13 (Mo $K\alpha$) | 18.74 (Mo $K\alpha$) |
| Diffractometer used | Syntex R3 | Syntex R3 |
| Radiation | Mo $K\alpha$ | Mo $K\alpha$ |
| $\lambda$/Å | 0.71073 | 0.71073 |
| Maximum $\theta$/° | 24.19 | 26.47 |
| Total reflections measured | 4129 | 9691 |
| Unique reflections | 4100 | 9680 |
| Function minimized was | $\sum\left[w(\lvert F_o\rvert^2-\lvert F_c\rvert^2)^2\right]$ which $w=\exp(5.0\sin^2\theta/\lambda^2)/\sigma^2(F_o)$ | $\sum\left[w(\lvert F_o\rvert^2-\lvert F_c\rvert^2)^2\right]$ which $w=\exp(5.0\sin^2\theta/\lambda^2)/\sigma^2(F_o)$ |
| Reflections used ($\lvert F\rvert>3.00(\sigma(F))$) | 1984 | 8954 |
| No. of variables | 249 | 1002 |
| Residuals: *R*; $R_w$ | 0.057; 0.058 | 0.049; 0.056 |
| Goodness of fit: *S* | 3.69 | 4.32 |
| Maximum shift/e.s.d. in final cycle | 0.06 | 0.39 |
| Maximum negative peak in final diff. map/e Å$^{-3}$ | −0.65 | −0.99 |
| Maximum positive peak in final diff. map/e Å$^{-3}$ | 0.93 | 1.15 |

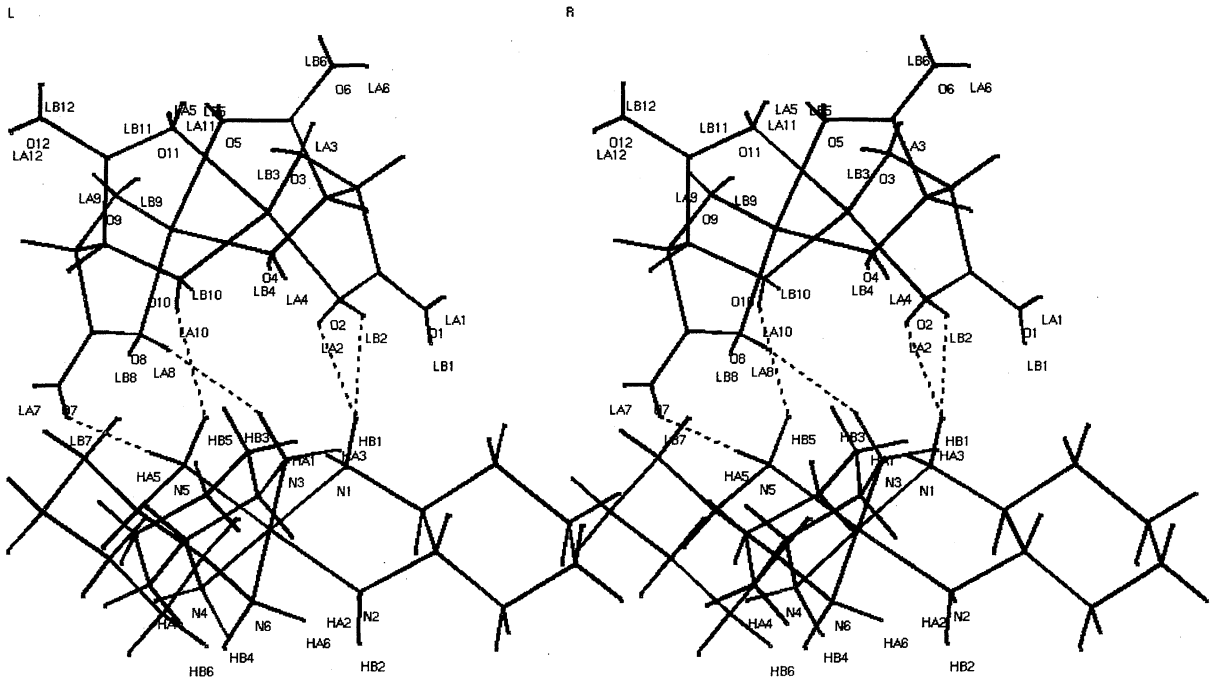


Fig. 3. Stereoscopic view of the *type-I* contact mode found in **1**. The lone-pairs are attached to the oxygen atoms and labeled as LA or LB. Hydrogen bonds are indicated as broken lines.

gen atoms[17] and the hydrogen bonds are indicated as broken lines. The geometrical parameters of these hydrogen bonds are summarized in Table 4.

In Fig. 3, the $[Sb_2(d\text{-tart})_2]^{2-}$ is bound to the complex with the four N–H···O bonds, i.e., N1–HB1···O2, N3–HB3···O8, N5–HB5···O10, and H5–HA5···O7, where N1–HB1···O2 is shared with the two lone-pairs LA2 and LB2 on O2. These hydrogen bonds are fairly different from those which we assumed in the previous section. It is true that the three lone-pairs (LB7, LA8, and LA10) are used for the hydrogen bonds, as in our proposal shown in Scheme 1, but are connected not with the three N–H groups on the $C_3$ site, but with two of them and one of the other N–H groups, N5–HA5; the remaining N–H group (N1–HB1) of the $C_3$ site is bound to the fourth O atom (O2). Among these four hydrogen bonds, the N···O distance of N3–HB3···LA8–O8, 3.47 Å, is rather larger than the others, and the H···L–O angle of N5–HA5···LB7–O7 is 109°, revealing that the lone-pair of O7 is not in a good direction to the N5–HA5 bond. The two shared hydrogen bonds of N1–HB1···O2 are also bent at the lone-pair position, though the N···O distance is the smallest among the four hydrogen bonds (Entries 1 through 4 in Table 4). As a result, the *type-I* interaction mode found here probably leads to a weaker overall interaction that expected in our assumed interaction mode. A much closer mode to ours, named as *type-II*, is discussed later. For the other contact mode in **1**, the geometrical parameters listed in the Entries 5—8 are very similar to those in the corresponding Entries 1—4, respectively, and were analyzed similarly.

In crystal **2**, since a crystallographically independent unit is found to be double of the formula, two $[Sb_2(d\text{-tart})_2]^{2-}$ and two $\Lambda\text{-}ob_3\text{-}[Co(chxn)_3]^{3+}$ are both independent in the crystal. The packing mode of these independent units is shown in Fig. 4, where one complex of the neighboring unit is included for the facile discussion (the bottom one). The alternate pile of the $[Sb_2(d\text{-tart})_2]^{2-}$ and the $\Lambda\text{-}ob_3\text{-}[Co(chxn)_3]^{3+}$ is found in this case again, and each of the two $C_3$ sites of the complexes makes a similar contact with the $[Sb_2(d\text{-tart})_2]^{2-}$. Among the four modes found in Fig. 4, the two bear a close structural resemblance to those found in the crystal **1** and are thus indicated as *type-I*. The only minor difference is in the hydrogen bonds on the N3 or N9 atom, which corresponds to the N3 atom in Fig. 3. N3 in Fig. 3 forms a single hydrogen bond through its left N3–HB3 group with LA8–O8, whereas the corresponding N3 atom in **2** does through its right N3–HA3 group with LB1–O1 (see Entry 10 in Table 4). In addition, the N3···O1 distance of 3.138 Å (in Entry 10) is smaller than the corresponding value of 3.47 Å (in Entry 2), but the HA3···LB1–O1 angle of 123.0° (in Entry 10) reveals that this hydrogen bond is bent. For the other *type-I* contact mode in **2**, N9 (corresponding to N3 in Fig. 3) forms two weak hydrogen bonds through both of its N–H group; the geometrical parameters of these hydrogen bonds listed in Entries 14 and 15 indicate that the N9–HA9···LB13–O13 bond is considerably bent at the lone-pair position and the N9–HB9···LA20–O20 bond has a large N···O distance.

Other hydrogen bonds listed in Entries 9 and 13, 11 and 16, and 12 and 17 have similar geometrical parameters to those of the corresponding hydrogen bonds listed in Entries 1, 3, and 4, respectively. It is thus concluded that these two *type-I* modes found in **2** are roughly similar in strength to those found in **1**.

On the other hand, the two remaining contact modes shown as *type-II* in Fig. 4 are fairly different from the above-mentioned *type-I* contact modes, but are rather close to our model

Table 2. Selected Fractional Atomic Coordinates and Equivalent Isotropic Displacement Parameters ($U_{eq}$) of **1**

| Atom | $x$ | $y$ | $z$ | $U_{eq}$ (Å$^2$)[a)] |
|---|---|---|---|---|
| Sb1 | −0.1003 (2) | 0.2785 (2) | 0.4059 (1) | 0.045 (2) |
| Sb2 | −0.0966 (3) | 0.3379 (2) | 0.1793 (1) | 0.070 (2) |
| Co1 | 0.3982 (4) | 0.2961 (3) | 0.3374 (2) | 0.039 (2) |
| O1 | 0.081 (3) | 0.479 (2) | 0.368 (1) | 0.096 (9) |
| O2 | 0.0470 (19) | 0.3609 (15) | 0.3911 (9) | 0.060 (7) |
| O3 | −0.1884 (17) | 0.3577 (14) | 0.3609 (8) | 0.044 (5) |
| O4 | −0.0372 (19) | 0.4003 (16) | 0.2488 (10) | 0.062 (7) |
| O5 | −0.267 (2) | 0.384 (2) | 0.215 (1) | 0.070 (7) |
| O6 | −0.336 (2) | 0.475 (2) | 0.276 (1) | 0.076 (8) |
| O7 | 0.1382 (19) | 0.1602 (16) | 0.2195 (9) | 0.060 (6) |
| O8 | 0.072 (2) | 0.274 (2) | 0.198 (1) | 0.073 (7) |
| O9 | −0.1605 (19) | 0.2472 (14) | 0.2201 (9) | 0.056 (6) |
| O10 | −0.0132 (17) | 0.2266 (15) | 0.3361 (8) | 0.045 (5) |
| O11 | −0.2463 (18) | 0.2135 (16) | 0.3682 (9) | 0.055 (6) |
| O12 | −0.286 (3) | 0.120 (2) | 0.299 (1) | 0.091 (9) |
| N1 | 0.305 (2) | 0.333 (2) | 0.411 (1) | 0.050 (7) |
| N2 | 0.517 (2) | 0.375 (2) | 0.358 (1) | 0.051 (7) |
| N3 | 0.301 (2) | 0.365 (2) | 0.282 (1) | 0.058 (8) |
| N4 | 0.489 (2) | 0.268 (2) | 0.261 (1) | 0.056 (7) |
| N5 | 0.2786 (19) | 0.2150 (17) | 0.3286 (10) | 0.044 (6) |
| N6 | 0.494 (2) | 0.229 (2) | 0.389 (1) | 0.044 (6) |
| C1 | 0.385 (3) | 0.382 (2) | 0.448 (1) | 0.047 (8) |
| C2 | 0.323 (3) | 0.431 (3) | 0.495 (2) | 0.07 (1) |
| C3 | 0.423 (4) | 0.475 (2) | 0.531 (2) | 0.08 (1) |
| C4 | 0.501 (5) | 0.523 (3) | 0.483 (2) | 0.12 (2) |
| C5 | 0.559 (3) | 0.473 (2) | 0.439 (2) | 0.07 (1) |
| C6 | 0.462 (3) | 0.429 (2) | 0.405 (2) | 0.053 (8) |
| C7 | 0.364 (3) | 0.374 (2) | 0.222 (2) | 0.07 (1) |
| C8 | 0.295 (4) | 0.409 (3) | 0.167 (2) | 0.08 (1) |
| C9 | 0.367 (3) | 0.398 (3) | 0.106 (2) | 0.08 (1) |
| C10 | 0.419 (4) | 0.319 (3) | 0.088 (2) | 0.09 (1) |
| C11 | 0.496 (3) | 0.291 (3) | 0.144 (2) | 0.08 (1) |
| C12 | 0.419 (3) | 0.296 (2) | 0.205 (1) | 0.051 (8) |
| C13 | 0.334 (3) | 0.141 (2) | 0.352 (1) | 0.042 (7) |
| C14 | 0.239 (3) | 0.079 (2) | 0.370 (1) | 0.053 (9) |
| C15 | 0.307 (3) | 0.013 (2) | 0.397 (2) | 0.07 (1) |
| C16 | 0.379 (3) | 0.037 (2) | 0.454 (1) | 0.06 (1) |
| C17 | 0.477 (3) | 0.099 (2) | 0.436 (1) | 0.050 (9) |
| C18 | 0.408 (3) | 0.166 (2) | 0.410 (1) | 0.042 (6) |
| C19 | 0.012 (3) | 0.425 (3) | 0.372 (2) | 0.06 (1) |
| C20 | −0.127 (3) | 0.429 (2) | 0.350 (1) | 0.06 (1) |
| C21 | −0.119 (3) | 0.448 (2) | 0.280 (1) | 0.07 (1) |
| C22 | −0.255 (3) | 0.434 (2) | 0.256 (2) | 0.061 (9) |
| C23 | 0.057 (3) | 0.208 (2) | 0.213 (1) | 0.052 (8) |
| C24 | −0.077 (3) | 0.187 (2) | 0.233 (1) | 0.050 (8) |
| C25 | −0.081 (3) | 0.172 (2) | 0.302 (1) | 0.047 (8) |
| C26 | −0.214 (3) | 0.169 (3) | 0.324 (2) | 0.066 (9) |

a) $U_{eq} = 1/3 \sum_i \sum_j U_{ij} a_i^* a_j^* \boldsymbol{a}_i \cdot \boldsymbol{a}_j$.

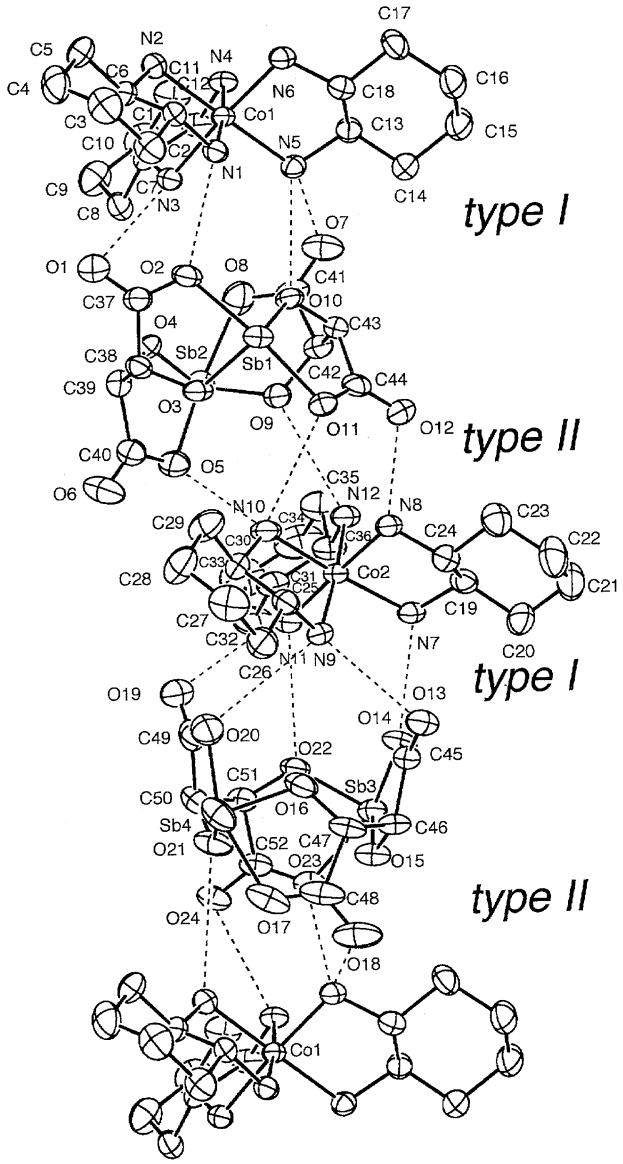


Fig. 4. Drawing of packing mode of $\Lambda$-*ob*$_3$-$[Co(chxn)_3]^{3+}$ and $[Sb_2(d\text{-tart})_2]^{2-}$ in **2**. The bottom complex (Co1) is of a neighboring asymmetric unit.

proposed. In the bottom *type-II* contact mode shown in Fig. 4, the three oxygen atoms, O21, O23, and O24, form the three hydrogen bonds with the three N–H groups at the $C_3$ site, N2–HB2, H6–HB6, and N4–HB4, respectively. The geometrical parameters in Entries 19 and 20 indicate that the lone-pairs of O23 and O24 are nicely directed to the N6–HB6 and N4–HB4 bonds, respectively, to form the two linear hydrogen bonds, while those in Entry 18 indicate that the lone-pair LA21 of O21 is directed off the N2–HB2 bond to form a weaker hydrogen bond bent at the lone-pair position. The additional hydrogen bond between O18 and N6–HA6 is also bent at the lone-pair position.

The other *type-II* contact mode is much closer to what we expect, as shown in the stereoscopic view of Fig. 5, where the linearity of the hydrogen bond is considerably improved for N12–HB12···LB9–O9 (135.6° in Entry 22), corresponding to the N2–HB2···LA21–O21 bond in the first *type-II* contact mode (124.9° in Entry 18). In addition, the N···O distance of 3.089 Å (in Entry 22) becomes significantly small compared to that (3.580 Å) in Entry 18, indicating that the hydrogen bond is by far stronger than in Entry 18. Furthermore, the linearity of the additional hydrogen bond (Entry 25) becomes much better than in Entry 21, as indicated by their H···L–O angles. Consequently, all four hydrogen bonds in Fig. 5 are

Table 3. Selected Fractional Atomic Coordinates and Equivalent Isotropic Displacement Parameters ($U_{eq}$) of **2**

| Atom | $x$ | $y$ | $z$ | $U_{eq}$ (Å$^2$)[a)] | Atom | $x$ | $y$ | $z$ | $U_{eq}$ (Å$^2$)[a)] |
|---|---|---|---|---|---|---|---|---|---|
| Sb1 | 0.69310 (3) | 0.22300 | 0.23740 (2) | 0.0349 (2) | C6 | 1.0298 (5) | 0.0789 (5) | 0.4709 (4) | 0.038 (3) |
| Sb2 | 0.47020 (4) | −0.00790 (4) | 0.25580 (3) | 0.0457 (3) | C7 | 0.7664 (5) | −0.0396 (4) | 0.4824 (3) | 0.032 (3) |
| Sb3 | −0.04360 (3) | 0.19750 (4) | −0.17330 (2) | 0.0359 (2) | C8 | 0.6980 (6) | −0.0990 (4) | 0.4375 (4) | 0.040 (3) |
| Sb4 | 0.26510 (4) | 0.17430 (5) | −0.30380 (3) | 0.0549 (3) | C9 | 0.6850 (7) | −0.1707 (5) | 0.4862 (6) | 0.055 (4) |
| Co1 | 0.83900 (6) | 0.11580 (6) | 0.51240 (4) | 0.0270 (4) | C10 | 0.6444 (8) | −0.1477 (6) | 0.5588 (5) | 0.059 (5) |
| Co2 | 0.30090 (6) | 0.22700 (6) | 0.04120 (4) | 0.0301 (4) | C11 | 0.7097 (7) | −0.0832 (5) | 0.6022 (4) | 0.048 (4) |
| O1 | 0.8500 (5) | 0.0168 (4) | 0.2800 (3) | 0.058 (3) | C12 | 0.7203 (5) | −0.0131 (5) | 0.5505 (3) | 0.035 (3) |
| O2 | 0.7966 (4) | 0.1375 (3) | 0.2886 (3) | 0.041 (3) | C13 | 0.6988 (5) | 0.2315 (4) | 0.5475 (3) | 0.034 (3) |
| O3 | 0.6557 (4) | 0.1321 (3) | 0.1724 (3) | 0.038 (2) | C14 | 0.6184 (6) | 0.2921 (5) | 0.5237 (5) | 0.049 (4) |
| O4 | 0.6186 (3) | −0.0095 (3) | 0.2562 (2) | 0.027 (2) | C15 | 0.6165 (7) | 0.3503 (6) | 0.5876 (6) | 0.058 (5) |
| O5 | 0.4761 (4) | 0.0087 (3) | 0.1386 (3) | 0.048 (3) | C16 | 0.7198 (7) | 0.3874 (5) | 0.6091 (5) | 0.055 (4) |
| O6 | 0.5829 (5) | −0.0090 (5) | 0.0561 (3) | 0.067 (4) | C17 | 0.8018 (6) | 0.3254 (5) | 0.6332 (5) | 0.047 (4) |
| O7 | 0.4990 (5) | 0.1208 (4) | 0.4523 (3) | 0.057 (4) | C18 | 0.8033 (5) | 0.2669 (4) | 0.5688 (4) | 0.035 (3) |
| O8 | 0.5112 (5) | 0.0245 (4) | 0.3720 (3) | 0.059 (4) | C19 | 0.1831 (5) | 0.3591 (5) | 0.0751 (4) | 0.036 (3) |
| O9 | 0.4398 (4) | 0.1060 (3) | 0.2532 (3) | 0.039 (2) | C20 | 0.1005 (6) | 0.4187 (6) | 0.0507 (5) | 0.052 (4) |
| O10 | 0.6219 (3) | 0.1943 (3) | 0.3244 (2) | 0.036 (2) | C21 | 0.1218 (7) | 0.4917 (6) | 0.0969 (6) | 0.062 (5) |
| O11 | 0.5385 (4) | 0.2638 (3) | 0.1979 (3) | 0.040 (2) | C22 | 0.2263 (8) | 0.5244 (6) | 0.0908 (7) | 0.068 (6) |
| O12 | 0.3956 (4) | 0.2933 (4) | 0.2436 (3) | 0.049 (3) | C23 | 0.3104 (7) | 0.4655 (5) | 0.1139 (5) | 0.053 (4) |
| O13 | 0.1645 (5) | 0.3758 (3) | −0.1286 (3) | 0.047 (3) | C24 | 0.2867 (6) | 0.3909 (4) | 0.0667 (4) | 0.037 (3) |
| O14 | 0.0649 (4) | 0.2759 (3) | −0.1146 (3) | 0.044 (3) | C25 | 0.4400 (5) | 0.2676 (5) | −0.0587 (4) | 0.038 (3) |
| O15 | −0.0032 (4) | 0.2599 (4) | −0.2563 (3) | 0.044 (3) | C26 | 0.4724 (7) | 0.2814 (6) | −0.1331 (5) | 0.051 (4) |
| O16 | 0.2253 (5) | 0.2625 (4) | −0.2452 (3) | 0.050 (3) | C27 | 0.5906 (8) | 0.2869 (7) | −0.1218 (5) | 0.065 (5) |
| O17 | 0.1498 (6) | 0.2306 (5) | −0.3846 (3) | 0.066 (4) | C28 | 0.6383 (7) | 0.2149 (7) | −0.0832 (6) | 0.067 (6) |
| O18 | 0.0513 (6) | 0.3334 (6) | −0.4011 (3) | 0.075 (5) | C29 | 0.5998 (6) | 0.2003 (7) | −0.0077 (5) | 0.058 (5) |
| O19 | 0.2730 (5) | 0.0235 (4) | −0.1230 (3) | 0.058 (3) | C30 | 0.4826 (5) | 0.1928 (5) | −0.0208 (4) | 0.040 (3) |
| O20 | 0.3064 (4) | 0.1253 (4) | −0.1922 (3) | 0.056 (3) | C31 | 0.2276 (6) | 0.0720 (5) | 0.0582 (4) | 0.043 (4) |
| O21 | 0.1522 (4) | 0.1005 (4) | −0.2997 (3) | 0.053 (3) | C32 | 0.1488 (8) | 0.0062 (6) | 0.0355 (5) | 0.062 (5) |
| O22 | 0.0706 (4) | 0.1226 (3) | −0.1542 (3) | 0.039 (3) | C33 | 0.1431 (10) | −0.0475 (7) | 0.1038 (8) | 0.079 (7) |
| O23 | −0.0825 (4) | 0.1133 (3) | −0.2648 (3) | 0.042 (3) | C34 | 0.1128 (8) | −0.0007 (8) | 0.1688 (7) | 0.078 (7) |
| O24 | −0.0414 (4) | −0.0051 (4) | −0.3017 (3) | 0.049 (3) | C35 | 0.1864 (7) | 0.0670 (7) | 0.1919 (5) | 0.061 (5) |
| N1 | 0.8987 (4) | 0.1729 (3) | 0.4353 (3) | 0.032 (3) | C36 | 0.1969 (6) | 0.1188 (5) | 0.1238 (4) | 0.044 (4) |
| N2 | 0.9747 (5) | 0.0660 (4) | 0.5351 (3) | 0.038 (3) | C37 | 0.7943 (5) | 0.0704 (5) | 0.2551 (4) | 0.039 (3) |
| N3 | 0.7872 (4) | 0.0318 (3) | 0.4403 (3) | 0.032 (3) | C38 | 0.7194 (5) | 0.0649 (5) | 0.1832 (3) | 0.037 (3) |
| N4 | 0.7853 (4) | 0.0504 (4) | 0.5580 (3) | 0.034 (3) | C39 | 0.6526 (6) | −0.0073 (5) | 0.1867 (4) | 0.040 (4) |
| N5 | 0.7090 (4) | 0.1716 (3) | 0.4893 (3) | 0.031 (2) | C40 | 0.5665 (6) | −0.0034 (5) | 0.1195 (4) | 0.046 (4) |
| N6 | 0.8764 (4) | 0.2010 (4) | 0.5852 (3) | 0.037 (3) | C41 | 0.4896 (5) | 0.0944 (5) | 0.3887 (4) | 0.044 (4) |
| N7 | 0.1706 (4) | 0.2839 (4) | 0.0343 (3) | 0.037 (3) | C42 | 0.4501 (5) | 0.1482 (5) | 0.3220 (4) | 0.038 (3) |
| N8 | 0.3583 (4) | 0.3257 (3) | 0.0877 (3) | 0.033 (3) | C43 | 0.5200 (5) | 0.2171 (4) | 0.3214 (3) | 0.036 (3) |
| N9 | 0.3261 (4) | 0.2621 (4) | −0.0600 (3) | 0.035 (3) | C44 | 0.4805 (6) | 0.2632 (4) | 0.2497 (4) | 0.038 (3) |
| N10 | 0.4386 (4) | 0.1821 (4) | 0.0502 (3) | 0.042 (3) | C45 | 0.1020 (6) | 0.3282 (4) | −0.1552 (4) | 0.037 (3) |
| N11 | 0.2359 (5) | 0.1298 (4) | −0.0017 (3) | 0.041 (3) | C46 | 0.0622 (6) | 0.3239 (5) | −0.2388 (4) | 0.040 (3) |
| N12 | 0.2750 (5) | 0.1825 (4) | 0.1382 (3) | 0.038 (3) | C47 | 0.1543 (7) | 0.3171 (5) | −0.2810 (4) | 0.046 (4) |
| C1 | 1.0122 (5) | 0.1633 (4) | 0.4457 (4) | 0.035 (3) | C48 | 0.1147 (7) | 0.2916 (7) | −0.3629 (4) | 0.057 (5) |
| C2 | 1.0586 (6) | 0.1815 (5) | 0.3755 (5) | 0.050 (4) | C49 | 0.2561 (6) | 0.0653 (5) | −0.1792 (5) | 0.048 (4) |
| C3 | 1.1738 (7) | 0.1636 (6) | 0.3926 (5) | 0.059 (5) | C50 | 0.1612 (6) | 0.0471 (5) | −0.2387 (4) | 0.042 (4) |
| C4 | 1.1931 (7) | 0.0803 (6) | 0.4181 (6) | 0.062 (5) | C51 | 0.0677 (5) | 0.0544 (5) | −0.1994 (4) | 0.037 (3) |
| C5 | 1.1446 (6) | 0.0618 (6) | 0.4872 (5) | 0.052 (4) | C52 | −0.0251 (6) | 0.0533 (5) | −0.2595 (4) | 0.039 (3) |

a) $U_{eq} = 1/3 \sum_i \sum_j U_{ij} a_i^* a_j^* \boldsymbol{a}_i \cdot \boldsymbol{a}_j$.

ideal in linearity and, as a result, the *type-II* contact mode shown in Fig. 5 is, we propose, the most probable one-to-one contact mode which $[Sb_2(d\text{-tart})_2]^{2-}$ and $\Lambda$-*ob*$_3$-$[Co(chxn)_3]^{3+}$ adopt in solution.

**Conclusion.** One of the contact modes found in the diastereomeric salt of $[Sb_2(d\text{-tart})_2]^{2-}$ and $\Lambda$-*ob*$_3$-$[Co(chxn)_3]^{3+}$ strongly supports our association model in which the three helical lone-pairs on the oxygen atoms of $[Sb_2(d\text{-tart})_2]^{2-}$ are directed nicely to the three similarly helical N–H groups on the $C_3$ site of $\Lambda$-*ob*$_3$-$[Co(chxn)_3]^{3+}$. Based on this association model, the order of the affinity observed in the chromatography, $\Lambda$-*ob*$_3$ > $\Lambda$-*lel*$_3$ > $\Delta$-*lel*$_3$ > $\Delta$-*ob*$_3$, is rationally interpreted. This result suggests that the efficiency of the " lock and key" model for chiral discrimination is greatly improved when the directionality of the lone-pairs is incorporated into the discrimination mechanism. For example, those complexes which have only two helical N–H groups at appropriate sites are also discriminated by the two

Table 4. Geometrical Parameters for Hydrogen Bonds (N–H···L–O) Found in Contact Modes

| No. | N | H[a)] | L[b)] | O | N···O | H···O | ∠N–H···O | ∠N–H···L | ∠N···L–O |
|---|---|---|---|---|---|---|---|---|---|
| | | | | *type I* mode in crystal **1** | | | | | |
| 1 | N1 | HB1 | LA2 | O2 | 2.87 | 2.03 | 146 | 142 | 110 |
| | | | LB2 | | | | | 138 | 106 |
| 2 | N3 | HB3 | LA8 | O8 | 3.47 | 2.64 | 146 | 148 | 169 |
| 3 | N5 | HB5 | LA10 | O10 | 3.17 | 2.39 | 138 | 139 | 140 |
| 4 | N5 | HA5 | LB7 | O7 | 2.96 | 2.11 | 147 | 160 | 109 |
| | | | | *type I* mode in crystal **1** | | | | | |
| 5 | N6 | HB6 | LA11 | O11 | 2.86 | 2.08 | 138 | 133 | 119 |
| | | | LB11 | | | | | 130 | 97 |
| 6 | N4 | HB4 | LA5 | O5 | 3.50 | 2.63 | 150 | 152 | 167 |
| 7 | N2 | HB2 | LA3 | O3 | 3.21 | 2.41 | 140 | 142 | 144 |
| 8 | N2 | HA2 | LB6 | O6 | 2.97 | 2.12 | 147 | 162 | 104 |
| | | | | *type I* mode in crystal **2** | | | | | |
| 9 | N1 | HB1 | LA2 | O2 | 2.863 | 1.923 | 166.0 | 157.8 | 118.5 |
| | | | LB2 | | | | | 158.7 | 98.6 |
| 10 | N3 | HA3 | LB1 | O1 | 3.138 | 2.348 | 139.2 | 149.9 | 123.0 |
| 11 | N5 | HB3 | LA10 | O10 | 3.061 | 2.243 | 142.4 | 149.1 | 148.3 |
| 12 | N5 | HA5 | LA7 | O7 | 2.917 | 2.093 | 142.9 | 129.6 | 70.4 |
| | | | LB7 | | | | | 156.9 | 96.2 |
| | | | | *type I* mode in crystal **2** | | | | | |
| 13 | N7 | HB7 | LA14 | O14 | 2.853 | 1.948 | 156.3 | 146.7 | 111.8 |
| | | | LB14 | | | | | 149.0 | 99.7 |
| 14 | N9 | HA9 | LB13 | O13 | 3.033 | 2.185 | 146.6 | 150.5 | 111.8 |
| 15 | N9 | HB9 | LA20 | O20 | 3.328 | 2.434 | 154.5 | 156.3 | 172.9 |
| 16 | N11 | HB11 | LA22 | O22 | 3.272 | 2.492 | 138.3 | 140.9 | 132.1 |
| 17 | N11 | HA11 | LB19 | O19 | 2.944 | 2.123 | 142.6 | 153.4 | 112.9 |
| | | | | *type II* mode in crystal **2** | | | | | |
| 18 | N2 | HB2 | LA21 | O21 | 3.580 | 2.674 | 157.4 | 147.4 | 124.9 |
| 19 | N4 | HB4 | LB24 | O24 | 2.980 | 2.027 | 171.9 | 176.8 | 158.1 |
| 20 | N6 | HB6 | LA23 | O23 | 3.159 | 2.166 | 158.0 | 151.1 | 152.5 |
| 21 | N6 | HA6 | LB18 | O18 | 3.236 | 2.423 | 142.2 | 144.3 | 104.0 |
| | | | | *type II* mode in crystal **2** | | | | | |
| 22 | N12 | HB12 | LB9 | O9 | 3.089 | 2.172 | 159.4 | 148.9 | 135.6 |
| 23 | N8 | HB8 | LB12 | O12 | 2.842 | 1.889 | 171.3 | 176.8 | 155.4 |
| 24 | N10 | HB10 | LA11 | O11 | 3.134 | 2.202 | 163.2 | 160.1 | 163.4 |
| 25 | N10 | HA10 | LA5 | O5 | 3.373 | 2.483 | 154.2 | 149.6 | 153.4 |

a) The hydrogen atoms of each $NH_2$ group are labeled as HA and HB and located at the idealized position with 0.96 Å as a bond length. b) The two lone pairs of each oxygen atom are labeled as LA and LB and located at the tentative position with 0.6 Å as their length and with tetrahedral and trigonal angles for ether and carbonyl oxygen atoms, respectively.

helically oriented lone-pairs of $[Sb_2(d\text{-tart})_2]^{2-}$

## Experimental

**General Remarks.** The following complexes were prepared by the literature methods: *Λ*-*ob*$_3$-, *Δ*-*ob*$_3$-, *Λ*-*lel*$_3$-, and *Δ*-*lel*$_3$-[Co(chxn)$_3$]Cl$_3$,[18] [Co(diNOchar)]Cl$_3$, and [Co(NOsemichar)]Cl$_3$.[14] $K_2[Sb_2(d\text{-tart})_2]\cdot 3H_2O$ was commercially available and used without further purification.

**Chromatography.** The sample which are mixtures of equal amounts of the complexes are loaded on the top of a column (1×50 cm) packed with SP-Sephadex C-25 cation-exchange resin, and were eluted with saturated aqueous $K_2[Sb_2(d\text{-tart})_2]$ or 0.2 M $Na_2SO_4$ (1 M = 1 mol dm$^{-3}$). Each band was collected separately, and identified on the CD and UV-vis spectra.

**Preparation of *Λ*-*ob*$_3$-[Co(chxn)$_3$]Cl[Sb$_2$(*d*-tart)$_2$]·4.5H$_2$O (1).** $K_2[Sb_2(d\text{-tart})_2]\cdot 3H_2O$ (0.729 g, 1.09 mmol) in water (15 ml) was added slowly to *Λ*-*ob*$_3$-[Co(chxn)$_3$]Cl$_3$ (0.554 g, 1.09 mmol) dissolved in 10 ml of water. Thus-obtained fiber-like precipitates were filtered and redissolved into 100 ml of water. Very slow evaporation over a few weeks led to the formation of orange needle crystals. Since the crystals were very effloresce, the sample for the elemental analysis had lost a considerable amount of water of crystallization. Calcd for monohydrate $C_{26}H_{48}ClCoN_6O_{13}Sb_2$ (990.68): C, 31.52; H, 4.98; N, 8.49%. Found: C, 31.84; H, 4.88; N, 8.57%.

**Preparation of *Λ*-*ob*$_3$-[Co(chxn)$_3$](ClO$_4$)[Sb$_2$(*d*-tart)$_2$]·4H$_2$O (2).** To a solution of *Λ*-*ob*$_3$-[Co(chxn)$_3$]Cl$_3$ (0.501 g, 0.99 mmol) in 15 ml of water was added $NaClO_4$ until no further precipitates

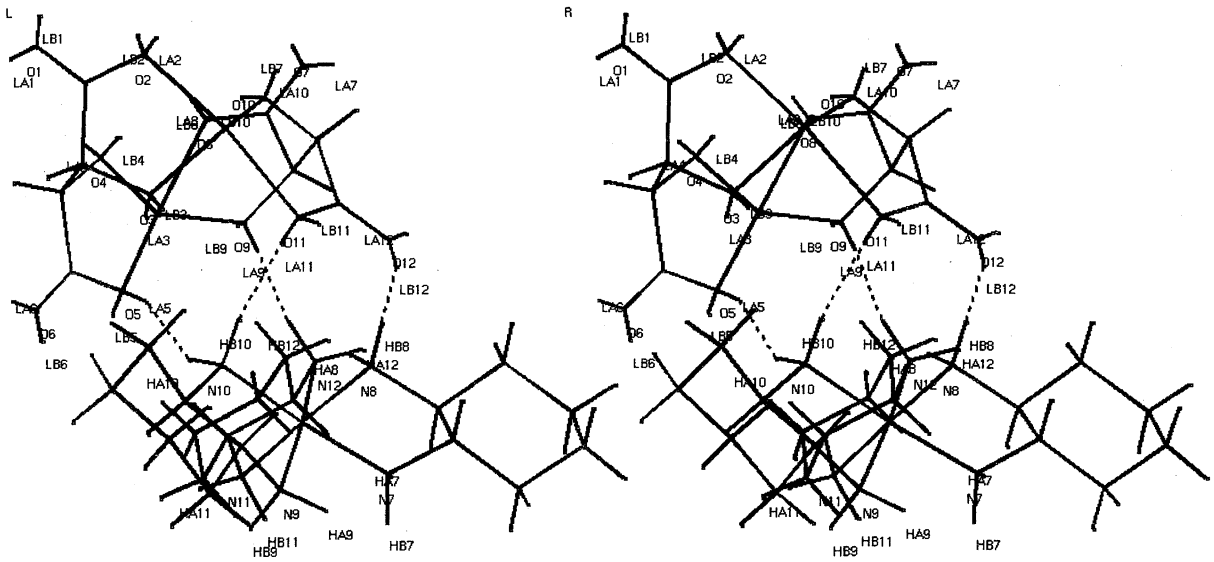

Fig. 5. Stereoscopic view of the *type-II* contact mode between $\Lambda$-*ob*$_3$-$[Co(chxn)_3]^{3+}$ (Co2) and $[Sb_2(d\text{-tart})_2]^{2-}$ (Sb1-Sb2) found in **2**. The lone-pairs are attached to the oxygen atoms and labeled as LA or LB. Hydrogen bonds are indicated as broken lines.

appeared. The precipitated $\Lambda$-*ob*$_3$-$[Co(chxn)_3](ClO_4)_3$ was redissolved in 50 ml of water. $Na_2[Sb_2(d\text{-tart})_2]\cdot 5H_2O$ (0.667 g, 0.99 mmol), prepared by a literature method,[19] was dissolved in 2 ml of water and added to the above complex solution. The orange plate crystals were obtained by slow evaporation of a mother liquor. Calcd for $C_{26}H_{54}ClCoN_6O_{20}Sb_2$ (1108.63): C, 28.17; H, 4.91; N, 7.58%. Found: C, 28.24; H, 4.56; N, 7.61%.

**X-Ray Crystallography.** Orange crystals of **1** and **2** were sealed in thin-walled capillaries, and mounted on a Syntex R3 diffractometer. The unit-cell dimensions were obtained from a least-squares fit of 25 reflections each for **1** ($10.9° \leq 2\theta \leq 24.5°$) and for **2** ($20.0° \leq 2\theta \leq 25.9°$). The reflection intensities were recorded by an $\omega$ scan at ambient temperature, and corrected for Lorentz and polarization effects. Three check reflections, measured after every 197 reflections, showed no decrease in intensity.

The structures were solved by a direct method with the program SIR92.[20] The thermal parameters ($U_{eqv}$) of oxygen atoms of some water molecules in both **1** and **2** amounted to unusually large values after several cycles of a full-matrix least-squares refinement, indicating disorder of the water molecules. The occupancy factors of these oxygen atoms were then reduced to appropriate values. All of the hydrogen atoms included in the calculation were placed at calculated positions by using a riding model (0.96 Å as a bond length). The available crystals for **1** were very small in size, and eventually the data for this compound were collected on an $0.1\times0.2\times0.4$ mm crystal. Since the scattering of the crystal was very weak, the number of available reflections was limited, resulting in a refinement with isotropic thermal parameters for the non-hydrogen atoms, except for Sb, Co, and Cl, which were treated anisotropically. For crystal **2**, the refinement was carried out with anisotropic thermal parameters for the non-hydrogen atoms, while the thermal parameters of the disordered atoms and the hydrogen atoms were treated isotropically.[21] An absorption correction was applied to **1**.[22] All calculations were performed using the Crystan 6.3 crystallographic software package.[23]

This work was supported by the Grant-in-Aid for Scientific Research Nos. 09740493 and 07404037 from the Ministry of Education, Science, Sports and Culture.

## References

1) A. G. Lappin and R. A. Marusak, *Coord. Chem. Rev.*, **109**, 125 (1991); D. A. Geselowits, A. Hammershoi, and H. Taube, *Inorg. Chem.*, **26**, 1842 (1987); S. E. Schadler, C. Sharp, and A. G. Lappin, *Inorg. Chem.*, **31**, 51 (1992); R. M. L. Warren, A. G. Lappin, and A. Tatehata, *Inorg. Chem.*, **31**, 1566 (1992); M. Iida, T. Nakamori, Y. Mizuno, and Y. Masuda, *J. Phys. Chem.*, **99**, 4347 (1995); M. Iida, Y. Mizuno, and N. Koine, *Bull. Chem. Soc. Jpn.*, **68**, 1337 (1995); J. P. Bolender, D. H. Metcalf, and F. S. Richardson, *Chem. Phys. Lett.*, **213**, 131 (1993); D. H. Metcalf, J. P. Bolender, M. S. Driver, and F. S. Rechardson, *J. Phys. Chem.*, **97**, 553 (1993); A. Tatehata and H. Akita, *Bull. Chem. Soc. Jpn.*, **64**, 1985 (1991); Y. Ohmori, M. Namba, Y. Kuroda, M. Kojima, and Y. Yoshikawa, *Inorg. Chem.*, **31**, 2299 (1992).

2) a) H. Yoneda, *J. Chromatogr.*, **313**, 59 (1984); b) K. Miyoshi, M. Natsubori, N. Dohmoto, S. Izumoto, and H. Yoneda, *Bull. Chem. Soc. Jpn.*, **58**, 1529 (1985); c) K. Miyoshi, Y. Sakamoto, A. Ohguni, and H. Yoneda, *Bull. Chem. Soc. Jpn.*, **58**, 2239 (1985); d) K. Miyoshi, N. Dohmoto, and H. Yoneda, *Inorg. Chem.*, **24**, 210 (1985); e) H. Yoneda, T. Yukimoto, Y. Kushi, and H. Nakazawa, *J. Liq. Chromotogr.*, **9**, 573 (1986); f) K. Miyoshi, S. Izumoto, K. Nakai, and H. Yoneda, *Inorg. Chem.*, **25**, 4654 (1986); g) K. Miyoshi, S. Izumoto, and H. Yoneda, *Bull. Chem. Soc. Jpn.*, **59**, 3475 (1986); h) H. Yoneda, U. Sakaguchi, and H. Nakazawa, *Bull. Chem. Soc. Jpn.*, **60**, 2283 (1987); i) H. Nakazawa, H. Ohtsuru, and H. Yoneda, *Bull. Chem. Soc. Jpn.*, **60**, 525 (1987); j) S. Izumoto, K. Miyoshi, and H. Yoneda, *Bull. Chem. Soc. Jpn.*, **60**, 3139 (1987).

3) a) T. Mizuta, K. Toshitani, K. Miyoshi, and H. Yoneda, *Inorg. Chem.*, **29**, 3020 (1990); b) T. Mizuta, K. Toshitani, and K. Miyoshi, *Inorg. Chem.*, **30**, 572 (1991); c) T. Mizuta, K. Toshitani, and K. Miyoshi, *Bull. Chem. Soc. Jpn.*, **64**, 1183 (1991); d) T. Mizuta and K. Miyoshi, *Bull. Chem. Soc. Jpn.*, **64**, 1859 (1991).

4) a) K. R. Butler and M. R. Snow, *J. Chem. Soc., Dalton Trans.*, **1976**, 251; b) A. Tatehata, M. Iiyoshi, and K. Kotsuji, *J. Am. Chem. Soc.*, **103**, 7391 (1981); c) M. Gajhede and S. Larsen, *Acta Crystallogr., Sect. B*, **B42**, 172 (1986); d) A. Tatehata and Y.

Asada, *Bull. Chem. Soc. Jpn.*, **61**, 3145 (1988); e) P. Osvath and A. G. Lappin, *Inorg. Chem.*, **26**, 195 (1987); f) R. A. Marusak, P. Osvath, M. Kemper, and A. G. Lappin, *Inorg. Chem.*, **28**, 1542 (1989); g) R. A. Marusak, C. Sharp, and A. G. Lappin, *Inorg. Chem.*, **29**, 4453 (1990).

5) T. Mizuta, A. Uchiyama, K. Ueda, K. Miyoshi, and H. Yoneda, *Chem. Lett.*, **1994**, 101.

6) a) L. C. Allen, *Proc. Natl. Acad. Sci., U.S.A.*, **72**, 4701 (1975); b) K. Morokuma, *Acc. Chem. Res.*, **10**, 294 (1977).

7) D. J. Millen, *J. Croat. Chem. Acta.*, **55**, 133 (1982).

8) a) R. Taylor and O. Kennard, *Acc. Chem. Res.*, **17**, 320 (1984); b) P. Murray-Rust and J. P. Glusker, *J. Am. Chem. Soc.*, **106**, 1018 (1984); c) A. Vedani and J. D. Dunits, *J. Am. Chem. Soc.*, **107**, 7653 (1985).

9) For recent reports: K. Yamanari, K. Okusako, and S. Kaisaki, *J. Chem. Soc., Dalton Trans.*, **1992**, 1615; H. Kanno, M. Tomita, S. Utsuno, and J. Fujita, *Bull. Chem. Soc. Jpn.*, **65**, 1233 (1992); K. J. Black, H. Huang, S. High, L. Starks, M. Olson, and M. E. McGuire, *Inorg. Chem.*, **32**, 5591 (1993); I. J. Clark, I. I. Creaser, L. M. Engelhardt, J. M. Harrowfield, E. R. Krausz, R. Elmars, G. M. Moran, A. M. Sargeson, and A. H. White, *Aust. J. Chem.*, **46**, 111 (1993); R. M. L. Warren, L. Oehrstroem, G. J. Gregory, M. Shang, and A. G. Lappin, *Inorg. Chim. Acta*, **225**, 75 (1994); T. Konno, Y. Kageyama, and K. Okamoto, *Bull. Chem. Soc. Jpn.*, **67**, 1957 (1994); A. H. Krotz and J. K. Barton, *Inorg. Chem.*, **33**, 1940 (1994); Y. Kageyama, T. Konno, K. Okamoto, and J. Hidaka, *Inorg. Chim. Acta*, **239**, 19 (1995); T. Konno, J. Hidaka, and K. Okamoto, *Bull. Chem. Soc. Jpn.*, **68**, 1353 (1995); K. Okamoto, Y. Kageyama, and T. Konno, *Bull. Chem. Soc. Jpn.*, **68**, 2573 (1995); T. J. Rutherford, M. G. Quagliotto, and F. R. Keene, *Inorg. Chem.*, **34**, 3857 (1995); R. T. Watson, J. L. Jackson, Jr., J. D. Harper, K. A. Kane-Maguire, L. A. P. Kane-Maguire, and N. A. P. Kane-Maguire, *Inorg. Chim. Acta*, **249**, 5 (1996); A. Derwahl, W. T. Robinson, and D. A. House, *Inorg. Chim. Acta*, **247**, 19 (1996).

10) Y. Yoshikawa and K. Yamasaki, *Coord. Chem. Rev.*, **28**, 205 (1979).

11) K. Nakajima, K. Tozaki, M. Kojima, and J. Fujita, *Bull. Chem. Soc. Jpn.*, **58**, 1130 (1985); Y. Yoshikawa, N. Kato, Y. Kimura, S. Utsuno, and G. N. Natu, *Bull. Chem. Soc. Jpn.*, **59**, 2123 (1986); S. Fanali, P. Masia, and L. Ossicini, *J. Chromatogr.*, **403**, 388 (1987); H. Umehara, T. Konno, K. Okamoto, and J. Hidaka, *Bull. Chem. Soc. Jpn.*, **60**, 1367 (1987); N. Koine, *Chem. Lett.*, **1988**, 1547; T. Konno, H. Umehara, K. Okamoto, and J. Hidaka, *Bull. Chem. Soc. Jpn.*, **62**, 3015 (1989); T. Fukuchi, N. Nagao, E. Miki, K. Mizumachi, and T. Ishimori, *Bull. Chem. Soc. Jpn.*, **62**, 2076 (1989); T. Konno, S. Aizawa, K. Okamoto, and J. Hidaka, *Bull. Chem. Soc. Jpn.*, **63**, 792 (1990); L. J. Charbonniere, G. Bernaridinelli, C. Piguet, A. M. Sargeson, and A. F. Williams, *J. Chem. Soc., Chem. Commun.*, **1994**, 1419; P. V. Bernhardt, R. Bramley, L. M. Engelhardt, J. M. Harrowfield, D. C. R. Hockless, B. R. Korybut-Daszkiewicz, E. R. Krausz, T. Morgan, and A. M. Sargeson, *Inorg. Chem.*, **34**, 3589 (1995); H. Kanno, S. Manriki, E. Yamazaki, S. Utsuno, and J. Fujita, *Bull. Chem. Soc. Jpn.*, **69**, 1981 (1996).

12) G. H. Searle, *Aust. J. Chem.*, **30**, 2625 (1977).

13) U. Sakaguchi, A. Tsuge, and H. Yoneda, *Inorg. Chem.*, **22**, 3745 (1983).

14) NOsemichar: *N*,*N*′,*N*″-[nitromethylidynetris(methylene)]-tris(*trans*-1,2-cyclohexanediamine); diNOchar: 1,12-dinitro-3,10,14,21,24,31-hexaazapentacyclo[10.10.10.$0^{4,9}$.$0^{15,20}$.$0^{25,30}$]-dotriacontane: R. J. Geue, M. G. McCarthy, and A. M. Sergson, *J. Am. Chem. Soc.*, **106**, 8282 (1984).

15) K. Ogino, *Bull. Chem. Soc. Jpn.*, **42**, 447 (1969); J. K. Beatie, *Acc. Chem. Res.*, **4**, 253 (1971); A. M. Bond, T. W. Hambley, D. R. Mann, and M. R. Snow, *Inorg. Chem.*, **26**, 2257 (1987).

16) Y. Yoshikawa, *Chem. Lett.*, **1980**, 1385, the author has proposed in his molecular mechanics calculation that oxo anions such as $SO_4^{2-}$, $PO_4^{3-}$, or tartrate form three bifurcated hydrogen bonds with the three N–H groups of $[Co(en)_3]^{3+}$. If so, it is because the *ob*$_3$ isomer forms only three single hydrogen bonds with the N–H groups that it is eluted after the *lel*$_3$ isomer (see also Ref. 3b).

17) The length of lone-pairs is tentatively set to 0.6 Å, which is adopted as a standard value in the program of MM written by Alinger for a molecular mechanics calculation.

18) S. E. Harnung, B. S. Sorensen, I. Creaser, H. Maegaard, U. Pfenningger, and C. E. Schaffer, *Inorg. Chem.*, **15**, 2123 (1976).

19) T. Tachibana, Ed. in chief, "Shinjikken Kagaku Kouza", Maruzen, Tokyo, Japan (1977), Vol. 8(III), p. 1605.

20) SIR92: A. Altomare, M. C. Burla, M. Camalli, M. Cascarano, C. Giacovazzo, A. Guagliardi, and G. Polidori, *J. Appl. Crystallogr.*, **27**, 435 (1994).

21) Lists of atomic coordinates for omitted non-hydrogen atoms, calculated atomic coordinates for hydrogen atoms, bond lengths and angles, and anisotropic thermal parameters are deposited as Document No. 71022 at the Office of the Editor of Bull. Chem. Soc. Jpn.

22) DIFABS: N. Walker and Stuart, *Acta Crystallogr., Sect. A*, **A39**, 158 (1983).

23) "Crystan 6.3: A computer program for the solution and refinement of crystal structures from X-ray diffraction data," MAC Science, Japan (1995).